Circularly-Polarized Monopolar Microstrip Antenna for Future Smart Mobility Communication

Seongmin Pyo
Department of Information and Communication Engineering
Hanbat National University
Daejeon, South Korea
spyo@edu.hanbat.ac.kr

Haechul Choi
Department of Intelligent MediaEngineering
Hanbat National University
Daejeon, South Korea
choihc@hanbat.ac.kr

***Abstract*—This work presents a new circularly polarized monopolar microstrip antenna for future smart mobility communication system. The proposed antenna consists of hexagonal quasi-circular patches on the top plane, complemented by asymmetric trapezoid slots on the ground. By integrating rotated asymmetric trapezoid ground slots, the antenna induces a radiation pattern characterized with right-handed circularly polarization. The parameters have been optimized by precise design considerations for enhanced performance.**

Keywords— ground slots, axial ratio, circular polarization, omnidirectional, quasi circular patch.

I. Introduction

Circularly polarized (CP) monopolar microstrip antennas with omnidirectional radiation patterns are widely employed in modern wireless communication systems due to their resistance against multipath distortion and polarization mismatch losses. Their capability to offer expanded signal coverage, improve signal transmission stability, and their adaptability for installation on moving vehicles further amplifies their effectiveness. Therefore, numerous studies have explored the realm of omnidirectional circularly polarized (CP) antennas.

In this research, our primary aim was to attain circular polarization in a quasi-circular arrangement of seven hexagonal patched monopolar microstrip antenna. To achieve this, we investigated a novel symmetric and asymmetric trapezoid ground slot structures. Then, the incorporation of asymmetrical trapezoid ground slots yielded right-handed circular polarization (RHCP). This structural enhancement contributes to the overall simplicity of the antenna design. The next sections will delve into specific aspects of the proposed antenna, including its configuration, parametric study, electric field distribution, reflection coefficient, radiation pattern, electrical characteristics.

II. Antenna Design and Analysis

A. Configuration of Proposed Antenna

The proposed antenna structure is depicted in Fig. 1. The antenna comprises a 1.575mm thick RT/Duroid 5880 substrate with a diameter of 86 mm, possessing a relative permittivity of 2.2 and a loss tangent of 0.001. To provide an omnidirectional radiation pattern, a hexagonal patch is positioned on the top plane of the substrate acts as a radiator, and directly connected to a 50-ohm coaxial line, along with six patches arranged in a quasi-circular shape.

This unique configuration, where the length of a single patch equals half the guided wavelength, results in the identification of the first yielding mode as the non-fundamental 1.5 wavelength resonant mode. On the bottom plane of the antenna, a conventional wire grounded structure is employed for control impedance matching, positioned opposite the center-feed patch. Additionally, quasi circular arranged six sections of rotated asymmetric trapezoid slots have been investigated for achieving a RHCP antenna.

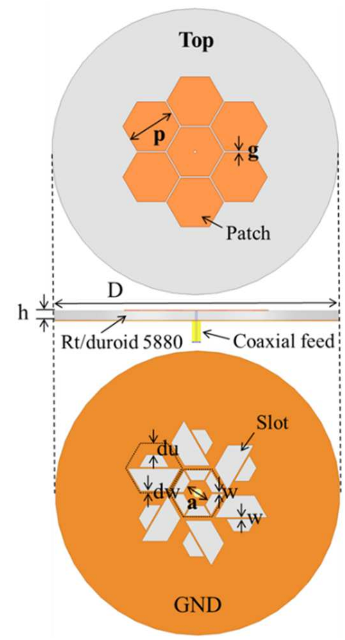

Fig. 1. Configuration of the proposed antenna.

TABLE I. Dimensions of the Proposed Antenna

Parameters	*Symbol*	*Value (mm)*
Patch length	p	12
Gap between patches	g	0.2
GND wire width	w	0.2
GND slot edge to patch edge distance 1	du	2
GND slot edge to patch edge distance 2	dw	0
GND middle hex. length	a	5
Substrate diameter	D	86
Substrate thickness	h	1.575

More details will be discussed in the next subsection. As illustrated in Fig. 1. the length of one hexagonal patch is adjusted to 12 mm, and the spacing between the hexagonal patches, along with the wire width, is chosen as 0.2 mm to ensure the stability of the manufacturing process. Therefore, a length of 5 mm is allocated for the middle hexagonal shape on the ground plane to provide ample soldering space for the coaxial feed. Detailed parameters are shown in Table 1.

B. *CP Design and Field Distribution*

Fig. 2. displays frequency responses for the proposed monopolar microstrip antenna with various ground slot structures. Firstly, we explored the frequency response of the initial symmetric trapezoid ground slot structure highlighted in red. The trapezoid ground slot exhibited significant influence on resonant mode, although no dual resonance phenomena were observed. To achieve circular polarization with a wider bandwidth for in the monopolar microstrip antenna, we introduced a 60-degree rotation in all six symmetrically arranged trapezoid slots. This modification resulted in an additional resonance frequency around 5.3 GHz, as shown in Fig. 2 and highlighted with a blue line.

Then, CP was successfully achieved proposed antenna with rotated asymmetric trapezoid slots, eliminating the need for additional shorting via structures. The parameters of antenna were optimized for the reflection coefficient highlighted with a black line in Fig. 2. This ground slot structure contributes to the proposed antenna's distinctiveness and simplicity.

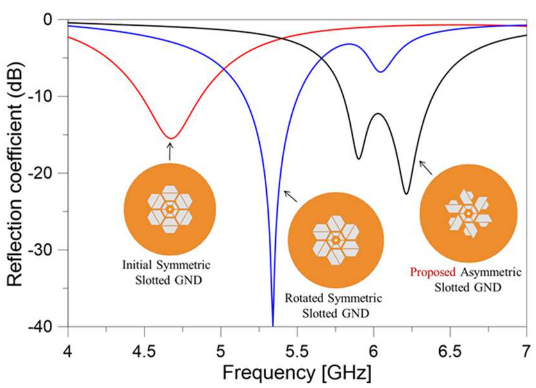

Fig. 2. Reflection coefficients of antennas with various trapezoid ground slot structures.

Fig. 3. illustrates simulated electric field distributions at two adjacent resonant frequencies of the proposed antenna at 5.9 GHz and 6.21 GHz.

C. *Parametric Study*

Fig. 4. presents parametric study variations in the reflection coefficient graph for different parameters of the proposed antenna. All dimensions have been chosen to attain the lowest frequency response value at the center frequency. On the other hand, values were selected to closely align with the resonant frequencies of the two adjacent TM02 modes. The following values for critical dimensions are as follows: substrate thickness (h)=1.575 mm, wire width (w)=0.2 mm, slot asymmetric distance (du)=2 mm, and length of middle hexagonal shape on the ground (a)=5 mm.

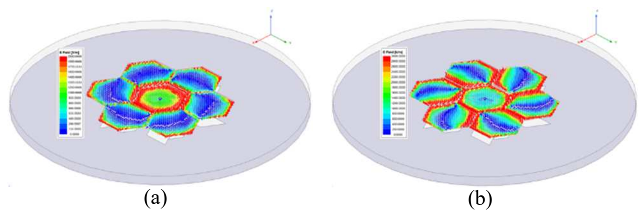

Fig. 3. Simulated electric field distributions of the TM02 modes (a) at 5.9 GHz and (b) at 6.21 GHz.

In Fig. 4(a) presents simulated frequency responses for the proposed antenna, exploring variations in substrate thickness denoted as h. The thickness h ranges 0.508 mm, 0.787 mm, and 1.575 mm, with a constant relative permittivity (εr) of 2.2 using a Roger RT/Duroid 5880 substrate. The results show that changes in substrate thickness influence dual resonant couplings, while the lower resonant mode consistently stays within the range of 5.8 GHz to 6 GHz. The substrate thickness plays a role in determining the upper resonant frequency with different coupling factors. When h is set to 1.575 mm, the simulation result clearly depicts two distinct resonant modes occurring at different frequencies, indicating a wide bandwidth and good impedance matching. Additional graphs in Fig. 4. show the influences of varying wire width, asymmetric size of the trapezoid slot, and the length of the middle hexagonal patch on the ground of the proposed antenna on the reflection coefficient. The parameter changes similarly affect both resonant frequencies. It is noteworthy that the center frequency response values are consistently higher than the chosen parameter values in all other three graphs.

III. IMPLEMENTATION AND SIMULATION RESULT

The optimization process aimed to achieve the lowest center frequency response while ensuring good impedance matching for two resonant frequencies. Detailed physical dimensions of the proposed antenna, fine-tuned during the optimization, are provided in Table 1.

Fig. 5 displays the simulated reflection coefficients of the proposed antenna. The results indicate a 10-dB impedance bandwidth spanning 590 MHz, ranging from 5.79 GHz to 6.38 GHz, corresponding to a 9.7% fractional bandwidth.

Fig. 6 shows the simulated axial ratio, as well as the realized RHCP gain of the microstrip antenna at $\phi=0^\circ$ and $\theta = 30^\circ$. Notably, the axial ratio closely approaches 0 dB at the center frequency and the antenna exhibits 3 dB AR bandwidths of approximately 81 MHz (1.3%) from 5.987 GHz to 6.068 GHz. The RHCP peak gain is observed to be 4.8 dBi around 6.02 GHz.

The RHCP and LHCP far field radiation pattern of the proposed antenna is presented in Fig.7 at 5.82 GHz. The radiation pattern reveals that the proposed antenna effectively demonstrated a RHCP omnidirectional radiation pattern.

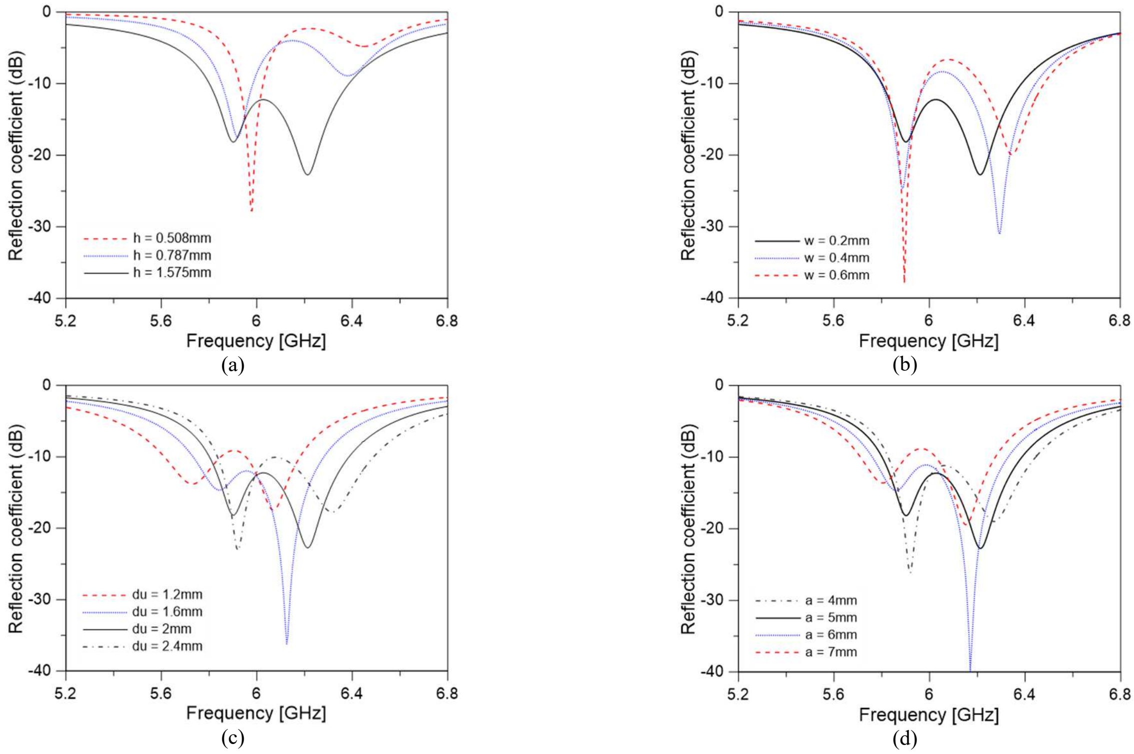

Fig. 4. The parametric study results for the proposed antenna (a) substrate thickness, (b) wire width, (c) slot to patch edge asymmetric distance change, and (d) middle hexagonal length on the ground.

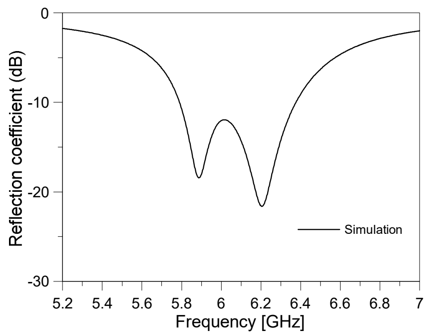

Fig. 5. Reflection coefficient of the proposed antenna.

The cross-polarization ratios, measuring the difference between the RHCP co-polarization and the LHCP cross-polarization, were consistently detected to be approximately 24 dB for the elevation plane at θ = 25˚. The radiation patterns were also simulated at other frequencies and stable results were obtained across the entire bandwidth.

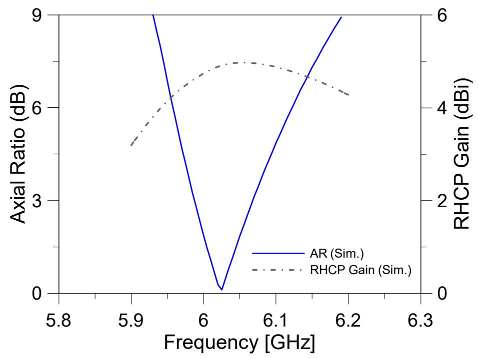

Fig. 6. Axial ratio and RHCP gain of the proposed antenna.

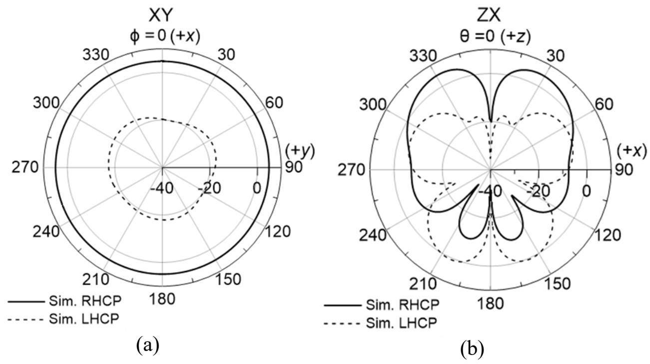

Fig. 7. Radiation patterns of the proposed antenna at center frequency 6.02 GHz (a) *H*-plane (xy-plane) ϕ=0˚ and (b) *E*-plane (zx-plane) θ = 30˚.

IV. Conclusion

This study presented the monopolar antenna design supported with circularly polarization. By integrating rotated asymmetric trapezoid ground slots, the proposed antenna induces RHCP operation. The proposed antenna may be a good candidate for future smart mobility communication due to the circular polarization radiation characteristics yielding a low surface drag and minimal multi-pass fading effect.

Acknowledgement

This work was supported by Korea Research Institute for defense Technology planning and advancement(KRIT) grant funded by the Korea government(DAPA(Defense Acquisition Program Administration)), 21-106-A00-007, Space-Layer Intelligent Communication Network Laboratory, 2022.

REFERENCES

[1] Y. M. Pan, K. W. Leung, and K. Lu, "Omnidirectional linearly and circularly polarized rectangular dielectric resonator antennas," IEEE Transactions on Antennas and Propagation, vol. 60, no. 2, pp. 751–759, Feb. 2012.

[2] H. Kawakami, G. Sato, and R. Wakabayashi, "Research on circularly polarized conical-beam antennas," IEEE Antennas and Propagation Magazine, vol. 39, pp. 27–39, Jun. 1997.

[3] Y. M. Pan and K. W. Leung, "Wideband circularly polarized dielectric bird-nest antenna with conical radiation pattern," IEEE Transactions on Antennas and Propagation, vol. 61, no. 2, pp. 563–570, 2013.

[4] D. Yu, S.-X. Gong, Y.-T. Wan, Y.-L. Yao, Y.-X. Xu, and F.-W. Wang, "Wideband omnidirectional circularly polarized patch antenna based on vortex slots and shorting vias," IEEE Transactions on Antennas and Propagation, vol. 62, no. 8, pp. 3970–3977, Aug. 2014.

[5] B. C. Park and J. H. Lee, "Omnidirectional circularly polarized antenna utilizing zeroth-order resonance of epsilon negative transmission line," IEEE Transactions on Antennas and Propagation, vol. 59, no. 7, pp. 2717–2721, 2011.

[6] K. Sun, L. Peng, and X. Jiang, "Design of a circularly polarized omnidirectional ZOR antenna for 5G millimeter wave", in Proceedings of the 2017 Sixth Asia-Pacific Conference on Antennas and Propagation, Xi'an, China, pp. 1-3, July 2018.

[7] Y. Liu, X. Li, L. Yang, and Y. Liu, "A Dual-Polarized Dual-Band Antenna with Omnidirectional Radiation Patterns," IEEE Transactions on Antennas and Propagation, vol. 65, no. 8, pp. 4259–4262, Aug. 2017.

[8] K. L. Lau and K. M. Luk, "A wideband circularly polarized conical beam patch antenna," IEEE Transactions on Antennas and Propagation, vol. 54, pp. 1591–1594, May 2006.

[9] J.-S. Row and M.-C. Chan, "Reconfigurable circularly-polarized patch antenna with conical beam," IEEE Transactions on Antennas and Propagation, vol. 58, no. 8, pp. 2753–2757, Aug. 2010.

[10] Y.-M. Cai, S. Gao, Y. Yin, W. Li, and Q. Luo, "Compact-size low-profile wideband circularly polarized omnidirectional patch antenna with reconfigurable polarizations," IEEE Transactions on Antennas and Propagation, vol. 64, no. 5, 2016.